ACS APPLIED BIO MATERIALS

www.acsabm.org Article

Serum Albumin Aggregation Facilitated by Cobalt and Chromium Metal Ions

Zoltan Wolfgang Richter-Bisson,* Aleksandra Doktor, and Yolanda Susanne Hedberg*

Cite This: ACS Appl. Bio Mater. 2023, 6, 3832−3841 Read Online

ACCESS | Metrics & More | Article Recommendations | Supporting Information

ABSTRACT: The interaction of serum proteins with cobalt (Co) and chromium (Cr) ions is poorly understood, but it is suspected to result in protein aggregation, which may alter the corrosion process of biomedical CoCr alloys or result in adverse health effects. Here, we study the aggregation ability and mechanism of bovine serum albumin (BSA) induced or accelerated by aqueous Co(II) and Cr(III) ions. The metal salts were selected by chemical speciation modeling, and they did not affect the pH or precipitate under simulated physiological conditions (150 mM NaCl and pH 7.3). The counterion of Cr(III) influenced the binding to BSA only at physiologically irrelevant low ionic strength. This study used a variety of spectroscopic and light scattering methods. It was determined that both metal ions and an equimolar mixture of metal ions have the potential to induce protein aggregation. Melting curves collected by circular dichroism spectroscopy indicate that Co(II) significantly reduced BSA's melting temperature when compared with Cr(III) or an equimolar mixture of Co(II) and Cr(III), both of which increased the melting temperature of BSA. The metal ions in solution preferentially interacted with BSA, resulting in the depletion of metal ions from the surrounding protein-free solution. Finally, this study suggests that the likely mechanism for Co(II)- and Cr(III)-induced BSA aggregation is salt bridging between protein molecules.

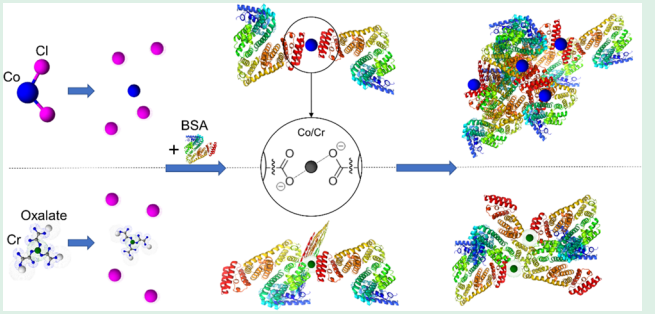

KEYWORDS: *bovine serum albumin (BSA), protein, aggregation, binding, bridging, protein−protein interaction*

1. INTRODUCTION

Civilization would not be possible without the use of multiple metals and alloys in the world around us; however, human health is impacted every day by metal contact, ranging from direct contact with metal surfaces to exposure to corrosion byproducts, nanoparticles, or ions.[1−4] The interaction of human proteins with these materials remains poorly understood, but metal−protein contact has been implicated as the cause of many adverse physiological reactions, such as allergies, contact dermatitis, pseudotumors, and cancer.[5−8] It has been suggested that metal exposure can result in structural changes and the aggregation of proteins, which in turn can influence interfacial corrosion reactions in protein-rich environments.[9,10] Protein aggregation is seen as harmful because it is toxic to cells[11] and thought to be the cause of many neurodegenerative diseases including Alzheimer's, Parkinson's, Huntington's, and amyotrophic lateral sclerosis (ALS).[8,12] Additionally, protein aggregation may result in reduced efficacy of protein-based pharmaceuticals due to their loss of structure and function.[8]

Cobalt (Co) and chromium (Cr) are two of the most common elements used in engineered alloys,[13] and contact hypersensitivity to these metals is extremely common.[9] While worn and corroding biomedical implants release these materials directly into the body,[14−16] environmental or dietary exposure will result in material passing through the skin or a mucous barrier, which may reduce their uptake, or they may experience detoxification by gut microbiota.[17] Many biomedical implants are alloys that consist of several metallic elements to improve function or reduce manufacturing costs. Corroding implants will release multiple constituent elements; therefore, it is important to understand the impact of different metal ions in synergy on protein aggregation. It is presumed that combinations of metals will increase protein aggregation, especially when one of the constituents is a trivalent metal species, such as Cr^{III}.[18] Cobalt−chromium (CoCr) alloys are common biomedical alloys that possess excellent wear resistance and hardness because of the cobalt, and good corrosion resistance from the chromium, which forms a protective surface oxide.[13,19,20] It is known that implants of this composition can contribute to a complication called aseptic lymphocyte-dominated vasculitis-associated lesions (ALVAL),

Received: June 28, 2023
Accepted: August 9, 2023
Published: August 23, 2023

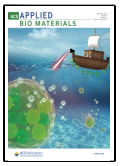

https://doi.org/10.1021/acsabm.3c00463
ACS Appl. Bio Mater. 2023, 6, 3832−3841

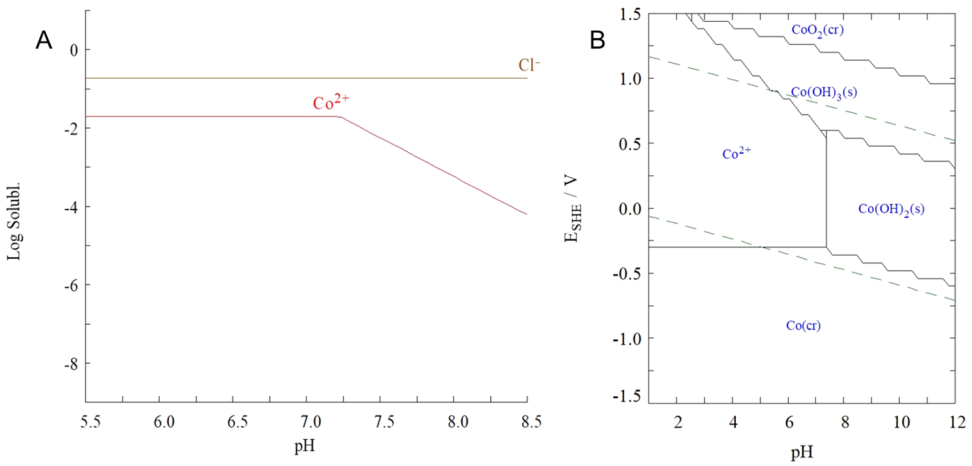

Figure 1. (A) Co^{II} solubility and (B) Co^{II} electrochemical stability (Pourbaix) diagram. System modeled using Hydra/Medusa,[39] $[Co^{2+}]_{tot}$ = 20.00 mM, ionic strength I = 0.150 M, $[Cl^-]_{tot}$ = 190.00 mM, T = 25 °C.

which is a type IV metal hypersensitivity response around the replaced joints.[21] The effects of biomedical implant (tribo)-corrosion are not necessarily localized: released metal ions and other mobile species, such as complexes and small nanoparticles, can dispense into the surrounding fluids and tissues or reach the circulatory system, where they are transported through the body to remote organs. A systematic review of 104 studies, totaling 9957 hip arthroplasty patients reported that mean concentrations of Co^{II} and Cr^{III} were increased in whole blood, serum, plasma, erythrocytes, and urine following implantation with a CoCr biomedical implant.[22]

Human serum albumin is a plasma protein that serves as a versatile carrier of metal ions. It has been described as the main carrier of Co^{II} in the blood.[23] Albumin proteins make up 60−65% of mammalian blood and serve to transport molecules such as fatty acids, hormones, minerals, and drugs.[24] The aggregation of these proteins is highly problematic. Albumin is also found in the synovial fluid, where it adsorbs to joint material surfaces and serves as a lubricant at a concentration of 11−13 mg/mL, roughly a third of the concentration in blood plasma. This functionality is of high interest for orthopedic implants.[25−27] In addition, the skin contains about 41% of the total extravascular albumin,[28] which could aggregate upon skin−metal contact. Ultimately, this makes albumin a desirable protein to study when exploring metal-induced protein aggregation. Bovine serum albumin (BSA) was selected as a relevant albumin model due to its 76% structural homology with human serum albumin, low cost, and wide availability.[29] BSA is also used as a model protein for biomedical implant safety tests, including biocompatibility, corrosion, and toxicity tests, meaning understanding its aggregation behavior is critical to understanding the outcome of these tests.[30−32]

The toxicity of a given metal is dependent on its physicochemical properties and ligand preferences. Chromium is a "hard" transition metal, so it favors binding to oxygen when in higher oxidation states such as Cr^{VI}, and sulfur in lower oxidation states such as Cr^{III}, although the binding of Cr^{III} to hard bases such as carbonates, carboxylates, or alcohols is also possible.[33,34] Cobalt is a borderline metal that may use oxygen, sulfur, or nitrogen as a ligand.[33] The major metal ions released from CoCr-based implants are Co^{II} and Cr^{III}, not the highly carcinogenic Cr^{VI}.[22] General consensus holds that proteins are the prime targets of heavy-metal species at physiologically relevant pH conditions, but the exact nature of this interaction or the mechanism by which metal ions promote protein aggregation is unclear. Several possible pathways exist for this phenomenon *in vivo*. Metals may interfere with the folding of nascent or non-native proteins, bind to free thiols or other functional groups in proteins, which may result in interprotein salt bridging, displace essential metal ions in metalloproteins, or catalyze the oxidation of amino acid side chains.[33−36] The pathways of relevance for metal-induced protein aggregation are suspected to be the disruption of the native structure, leading to partially unfolded intermediates that aggregate, or the formation of metal−ligand complexes with charged functional side chain groups, leading to salt bridging between different proteins.

Our hypothesis is that cobalt (Co) and chromium (Cr) ions of relevance for implant materials accelerate the aggregation of bovine serum albumin (BSA) by means of a salt-bridging mechanism. Confirmation of this hypothesis will be accomplished using inductively coupled plasma mass spectrometry (ICP-MS), scanning electron microscopy/energy-dispersive X-ray spectroscopy (SEM/EDS), circular dichroism (CD) spectroscopy, dynamic light scattering (DLS), and electrophoretic mobility (ζ-potential) measurements.

2. EXPERIMENTAL SECTION

2.1. Chemicals and Solutions. The solvent for all solutions was ultrapure (type 1) water purified with a Milli-Q Reference System (Millipore Sigma) to give a resistivity of 18.2 MΩ·cm. Metal ion stock solutions of 2 and 20 mM were prepared using cobalt(II) chloride ($CoCl_2$, ultradry, 99.998% (metal basis), Fisher Scientific, Ottawa, Canada), and potassium chromium(III) oxalate trihydrate ($K_3Cr(C_2O_4)_3{\cdot}3H_2O$, 98%, Sigma-Aldrich). Metal salts were chosen to have no impact on the solution pH. Bovine serum albumin (BSA, heat shock fraction, pH 7, ≥98%, Sigma-Aldrich) solutions were created in concentrations ranging from 1 to 15 g/L in 150 mM NaCl and 20 mM 2-(*N*-morpholino)ethanesulfonic acid buffer (MES, low moisture content, ≥99% by titration, Sigma-Aldrich), pH 7.2−7.4 adjusted with 8 M NaOH. Protein concentrations vary between experiments to account for the sensitivity of different instruments. The molar ratio of metal:BSA was 0:1, 8:1, or 24:1, created using metal ion stock solutions or an equimolar mixture of two stock solutions. A previous study of metal binding to albumin suggested that aggregation starts at an 8:1 ratio of metal/protein.[37] The ratio of 24:1 was chosen as a "worst case" scenario to exaggerate the effects of metal ions on the protein; however, it has been documented that tissues adjacent to titanium implants contained metal in excess of 2000 mg/mL (while

https://doi.org/10.1021/acsabm.3c00463
ACS Appl. Bio Mater. 2023, 6, 3832−3841

albumin is found in concentrations of no more than 40 mg/mL, giving a ratio of >50:1) in extreme cases of metallosis.[38]

To ensure Co^{II} and Cr^{III} solubilities, $CoCl_2$ and $K_3Cr(C_2O_4)_3 \cdot 3H_2O$ were chosen as the sources of the metal ions. $CoCl_2$, which is rapidly converted to $Co(H_2O)_6^{2+}$ in aqueous solution, remains, according to Hydra/Medusa chemical equilibrium software soluble up until a pH of approximately 7.3, at which point solubility drops as Co^{II} begins to convert to $Co(OH)_2$(s) (Figure 1).[39] Buffer pH was 7.3, so there may be minor amounts of $Co(OH)_2$ nanoparticle formation, although this quantity is assumed to be negligible (see Section S1 in the Supporting Information). Most Cr^{III} compounds are not very soluble at physiological pH (see Section S2 in the Supporting Information); therefore, $K_3Cr(C_2O_4)_3 \cdot 3H_2O$ was employed as the source of chromium as oxalate species to ensure Cr solubility and limit its precipitation.[10,40]

2.2. Inductively Coupled Plasma Mass Spectrometry (ICP-MS). Sample preparation steps are illustrated in Section S3 in the Supporting Information. A MES buffer solution with 15 g/L (0.23 mM) BSA was prepared and allowed to equilibrate for 1 h at room temperature. Metal ion solutions were added such that the molar metal/protein ratio was 8:1. Samples were equilibrated at 37 °C for 24 h, then denatured in a 90 °C water bath for 1 h. The same procedure was used to create blank samples that did not contain metal. Samples were centrifuged, the supernatant was collected, the pellet was rinsed 3 times with ultrapure water, and the rinses were collected. Concentrated nitric acid was added to pellets, rinses, and supernatants, and all were digested using warm acid digestion until no visible precipitate remained. For comparison, another set of samples (consisting of both protein-metal samples and blanks, as well as protein-free samples and blanks) were divided evenly into the top and bottom fractions without any thermal aggregation and then digested using microwave digestion. Samples were analyzed on a Thermo Scientific iCAP Q inductively coupled plasma mass spectrometer using helium as a collision gas to determine the quantity of the metal ions in each fraction. All samples were made and analyzed in triplicate, with the average concentrations over the three runs being reported. The instrument was calibrated with six prepared standards (0, 1, 10, 40, 80, 120 μg/L) of a Co and Cr multistandard to create linear calibration curves (Co R^2 = 1.000, Cr R^2 = 1.000). The detection limits, defined as instrument detection limit plus background equivalent concentration, were 0.119 and 0.144 μg/L for Co and Cr, respectively. All analyzed samples exceeded the limit of detection significantly, blank sample concentration was below the limit of detection. To ensure that the sample concentration was within the calibration range, the samples were diluted with 2% HNO_3 and the dilution factor was accounted for. Quality control samples were analyzed after every fifth run and maximum uncertainties in quality control samples showed acceptable (<10% error) concentration variations. All measured concentrations (in μg/L) were multiplied by the individual dilution factors to obtain the sample concentrations.

2.3. Scanning Electron Microscopy/Energy-Dispersive X-ray Spectroscopy. MES buffer solution was used to prepare 15 g/L (0.23 mM) BSA samples and allowed to equilibrate for one h at room temperature. Metal ion solutions were added such that the metal/protein ratio was 8:1. Samples were equilibrated at 37 °C for 24 h, then denatured in a 90 °C water bath for 1 h. Samples were centrifuged, and the supernatant was discarded. The pellets were rinsed thoroughly 3 times with ultrapure water, and the rinses were discarded. Pellets were stored in acid-cleaned glass vials and placed in a desiccator for 4 days until dry. The samples were gold-sputtered and imaged on a Hitachi SU3500 SEM using an acceleration voltage of 25.0 kV and secondary electron detection mode. The working distance was between 9.4 and 10.2 mm.

2.4. Circular Dichroism (CD). Sample preparation steps are illustrated in Section S3 in the Supporting Information. Tris(hydroxymethane)aminomethane (20 mM, Tris, ACS reagent, ≥99.8%, Sigma-Aldrich; 100 mM NaCl; pH 7.2−7.4) adjusted with 5% HCl was used to prepare 1.0 g/L (0.015 mM) BSA samples allowed to equilibrate for 60 min at room temperature. Tris buffer was employed for CD measurements instead of MES to reduce the background noise of the sample. Samples were diluted with Tris buffer, a 20.0 mM metal ion stock solution, or ultrapure water to create blank samples to a final protein concentration of 0.25 g/L (0.004 mM). Samples were equilibrated at 37 °C for approximately 120 min and then analyzed in triplicate between 20 and 100 °C ramped at 1 °C/min on a Jasco J-810 spectropolarimeter (Easton, MD) with a 1 mm quartz cuvette. Unfolding profiles were generated by monitoring the CD signal at 222 nm. Unfolding profiles were analyzed using the following expression.

$$CD_{222\ nm} = \frac{(m_N T + y_N) + p_U * \exp\left(\frac{-\Delta G}{RT}\right)}{1 + \exp\left(\frac{-\Delta G}{RT}\right)} \quad (1)$$

where $(m_N T + y_N)$ represents the equation of the pretransition baseline. The high melting point of BSA means that the post-transition baseline is not always well defined; p_U represents the terminal data point. For samples with a well-defined post-transition baseline, the following equation is used: where $(m_U T + y_U)$ represents the equation of the post-transition baseline.

$$CD_{222\ nm} = \frac{(m_N T + y_N) + (m_U T + y_U)\exp\left(\frac{-\Delta G}{RT}\right)}{1 + \exp\left(\frac{-\Delta G}{RT}\right)} \quad (2)$$

Free energy of unfolding is defined as $\Delta G(T) = \Delta H\left(1 - \frac{T}{T_m}\right)$, where T_m is the melting point of the protein. The enthalpy of unfolding was assumed to be constant over the temperature range considered for these experiments.[41] Fraction unfolded is represented by the following equation:

$$f_U = \frac{\exp\left(\frac{-\Delta G}{RT}\right)}{1 + \exp\left(\frac{-\Delta G}{RT}\right)} \quad (3)$$

2.5. Dynamic Light Scattering (DLS). Sample preparation steps are illustrated in Section S3 in the Supporting Information. A MES buffer solution with 10 g/L (0.15 mM) BSA was prepared and allowed to equilibrate for 1 h at room temperature. Prepared solutions were centrifuged at 4000g for 30 s to remove any insoluble debris or dust. The purified BSA solution was used to make four 1 mL samples, and 20 mM metal ion solutions or ultrapure water for blanks were added such that the molar metal/protein ratio was 8:1. The samples were gently mixed and allowed to equilibrate for 5 min. Samples were heated in an 80 °C oven for 0, 0.25, 0.5, and 1.0 h and analyzed in triplicate by DLS (Litesizer 500, Anton Paar) at 25 °C with a 2 min equilibration time. Measurement angle was automatically determined, quality mode was automatic with a maximum number of runs of 60, and solvent was chosen as 154 mM NaCl with the material of interest being protein (refractive index of 1.3318 and 1.4500, respectively, viscosity of 0.0009064 Pa × s, and protein absorption index of 0.0010).

2.6. ζ-Potential Measurement. MES buffer solution with 10 g/L (0.15 mM) BSA was prepared and allowed to equilibrate for 1 h at room temperature. 1.5 mL was transferred to a clean, dry microcentrifuge tube and centrifuged at 4000g for 30 s to remove any insoluble debris and dust. The top 1 mL was transferred to a different microcentrifuge tube containing 0.06 mL of 20 mM metal ion stock solution or ultrapure water, corresponding to an 8:1 metal/protein ratio. The solution was equilibrated at 37 °C for 2 h and analyzed in triplicate on the Litesizer 500 (Anton Paar), which can measure high-conductivity ζ-potential using their patented cmPALS technique (continuously monitored phase analysis light scattering, which is a form of electrophoresis) at 21 °C and a 1 min equilibration time. A Smoluchowski approximation was used, leading to a Henry factor of 1.5, power adjustment was automatic with a maximum potential of 200.0 V, the quality mode was automatic with the maximum number of runs of 1000, and the solvent was water (refractive index of 1.3306, a viscosity of 0.0009779 Pa × s, and a relative permittivity of 79.81).

https://doi.org/10.1021/acsabm.3c00463
ACS Appl. Bio Mater. 2023, 6, 3832−3841

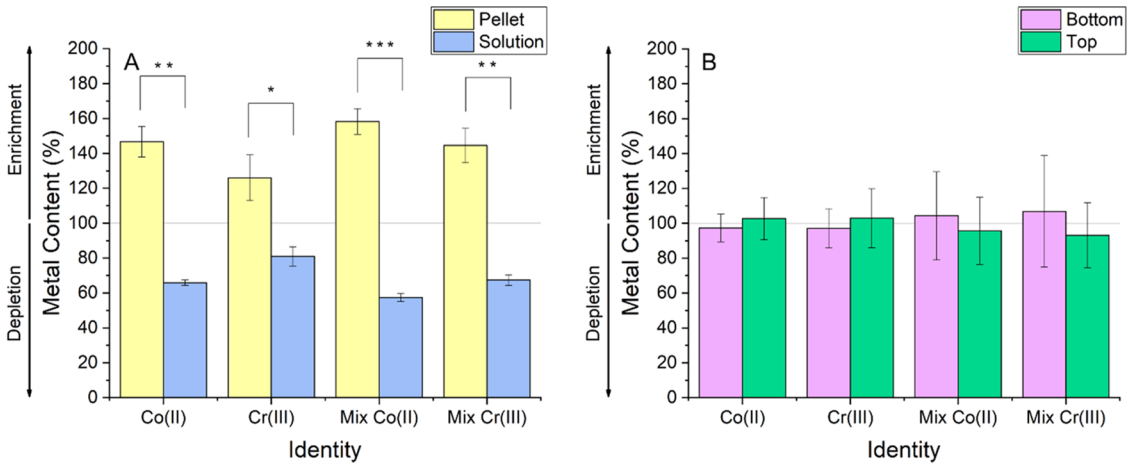

Figure 2. (A) Percent of metal ions found in thermally aggregated BSA pellet, as determined by ICP-MS analysis, normalized to the expected value from a homogeneous distribution of metals. (B) Percent of metal ions found in the top and bottom fractions of BSA solution incubated at room temperature with 8:1 metal ions, normalized to the expected value from a homogeneous distribution of metal, as determined by ICP-MS analysis (*$p \leq 0.05$; **$p \leq 0.01$; ***$p \leq 0.001$; between top and bottom fractions).

2.7. Statistical Analysis. To determine statistically significant differences between two sets of raw data, a two-tailed Student's *t*-test was used. If the probability (p) that these sets of data were equal was smaller than 0.05, then they were considered statistically different.

3. RESULTS AND DISCUSSION

3.1. ICP-MS. It was determined that the metal ions in the physiological solution were more likely to be found within thermally unfolded protein aggregate pellets than in the surrounding solution. The denatured protein pellets were determined to represent 42.2 ± 1.9% of the solutions by mass; however, 61.9 ± 6.0% of the Co^{II} ions in the cobalt-containing solution were found within the aggregated pellet. Likewise, 53.2 ± 10.4% of the Cr^{III} ions was found within the pellets. For solutions containing a mixture of both Co^{II} and Cr^{III}, 66.8 ± 4.7% of the Co and 61.0 ± 6.7% of the Cr were found in the pellet. All of these are statistically significant increases over the 42.2% expected from a homogeneous distribution of metals.

These results demonstrate that there is an affinity for the metal ions for the protein, especially when combinations of metal ions are present. Previous work suggested that combinations of metal ions will have a larger impact on protein aggregation than individual metal ions.[18,42−44] This synergistic effect is clearly seen in Figure 2A, where samples containing a combination of Co^{II} and Cr^{III} resulted in a higher percent of metal ions being incorporated in the protein pellet than their corresponding individual samples ($p = 0.021$ for Co^{II} samples; $p = 0.085$ for Cr^{III} samples). The absence of a concentration gradient before thermal aggregation of BSA (Figure 2B) suggests that there are a limited number of metal−protein colloids that precipitate out of solution. If this was the case, there would be an enrichment of metal in the bottom fraction; however, there were no statistically significant differences between top and bottom fractions. It was also experimentally determined there was no concentration gradient between the top and bottom fractions in protein-free samples.

3.2. SEM/EDS. EDS mapping was used to further verify the presence of metals within dried BSA aggregates and investigate their distribution. Co and chlorine (Cl) were detected for the Co samples, Cr and potassium (K) were detected for the Cr-containing samples, and Co, Cl, Cr, and K were detected for the mixture. These elements represent the constituent ions of the metal salts used in this study. Their distribution was relatively homogeneous, and for the mixtures, Co and Cr were co-detected in the same spots (Figure 3). There is a bright,

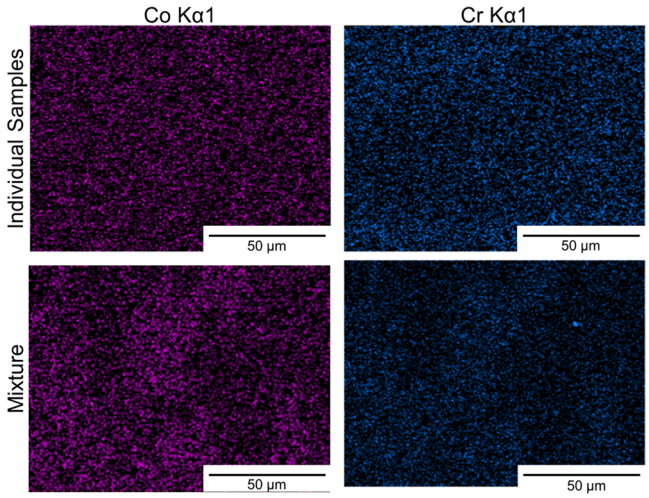

Figure 3. EDS images of BSA + Co^{II} (top left), BSA + Cr^{III} (top right), and BSA + Co^{II}/Cr^{III} (Co, bottom left; Cr, bottom right) mixture samples. The color intensity shows the relative presence of elements and is not a measure of the quantity across images.

high-intensity spot in the Cr mixture image, indicating a localized enrichment of Cr; however, this is not seen in other samples or EDS images suggesting this is a localized phenomenon and not representative of the distribution of metal ions across all samples.

3.3. Circular Dichroism (CD). The addition of metal ions resulted in extremely minor changes to the unfolding profile of BSA. To exaggerate the effects of metal ions on BSA's secondary structure, a metal/protein ratio of 24:1 was chosen as the starting point for CD measurement rather than 8:1. At the ratio of 24:1, Co slightly reduced the melting temperature, and Cr and the Co−Cr mixture both slightly increased the melting temperature. This is seen in Figure 4A. To determine if there is a concentration dependence of this trend, the melting

https://doi.org/10.1021/acsabm.3c00463
ACS Appl. Bio Mater. 2023, 6, 3832−3841

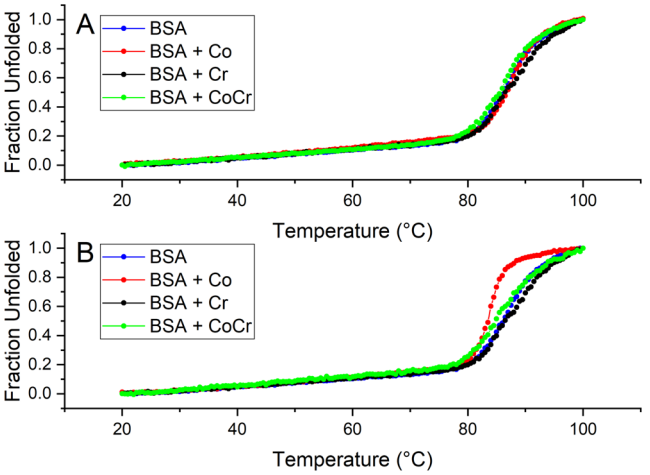

Figure 4. Fraction unfolded curves of BSA and (A) 24:1 metal ions and (B) large excess of metal ions (320:1) generated by CD spectroscopy at 222 nm.

curves were gathered again using a large excess of 320 mol equiv of metal, pictured in Figure 4B. The impacts of Co and Cr ions on the melting profile depended on concentration, with the melting temperature reducing from 85.4 ± 2.0 to 82.0 ± 2.2 °C (p = 0.061) in the presence of Co and increasing to 87.9 ± 0.72 °C (p = 0.060) in the presence of the Co−Cr mixture. The melting curve of Cr did not exhibit significant concentration dependence, and the melting temperatures were only mildly increased to 86.2 ± 1.9 (p = 0.33). The difference between the melting temperatures in the presence of Co(II) and those of Cr(III) and the mixture was statistically significant (p = 0.033 and 0.0058, respectively).

Equations 1 and 2 both describe their respective melting profiles very well (see Section S4 in the Supporting Information). This equation is based on a two-state model,[41] meaning that the thermally induced breakdown of BSA's helical structure can be approximated as a direct N → U (native to unfolded) two-state process with no partially unfolded intermediates. This suggests that the most likely mechanism for Co^{II} and Cr^{III}-induced BSA aggregation involves the chelation of metal ions by protein surface functional groups. The result is multiple proteins bridged together by metal ions, leading to a large tangle of proteins and metal ions. This is supported by our previous work which suggests that metal-induced albumin aggregates do not undergo loss of secondary structure; there was no change in the far UV CD signal of BSA upon the addition of metal salts, and ANS fluorescence revealed only minor changes in the signal of metal-containing and metal-free samples.[18]

3.4. Dynamic Light Scattering (DLS). DLS analysis of metal-free BSA solutions revealed that the average particle size increased following heating at 80 °C (Figure 5A), to a maximum size of 45.7 nm after one h of thermal incubation. All solutions containing metals were in an 8:1 metal/protein ratio. Size distribution measurements indicated that the presence of Co^{II} ions resulted in an increase (p values of 0.0037, 0.10, 0.25, and 0.0013 after 0, 0.25, 0.5, and 1 h, respectively) in the average particle size immediately after thermal incubation. This increase grew with longer durations of thermal incubation, with a maximal increase of particle size to 6910 nm after one h of heating. This is consistent with the

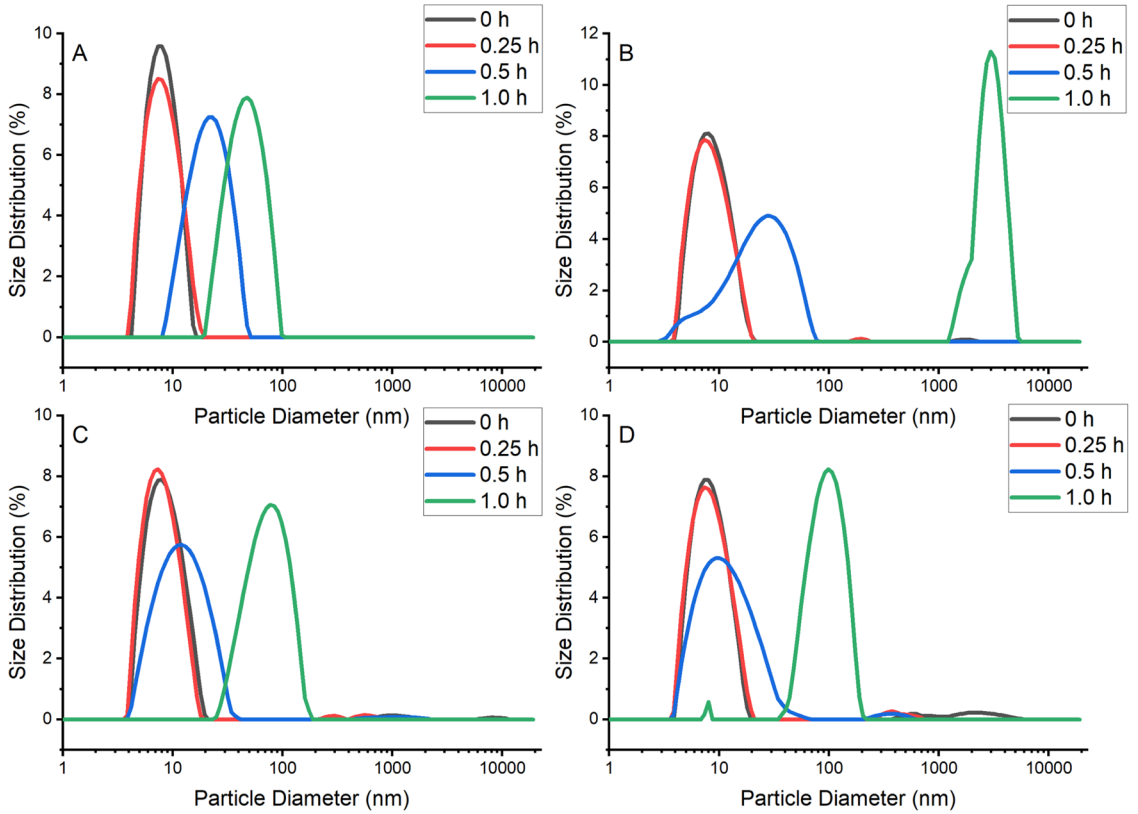

Figure 5. DLS analysis with an 8:1 metal/protein ratio showing representative curves of surface-mean diameter distribution by intensity of BSA at different 80 °C heating times: (A) native BSA, (B) BSA + Co^{II}, (C) BSA + Cr^{III}, and (D) BSA + $Co^{II}Cr^{III}$.

https://doi.org/10.1021/acsabm.3c00463
ACS Appl. Bio Mater. 2023, 6, 3832−3841

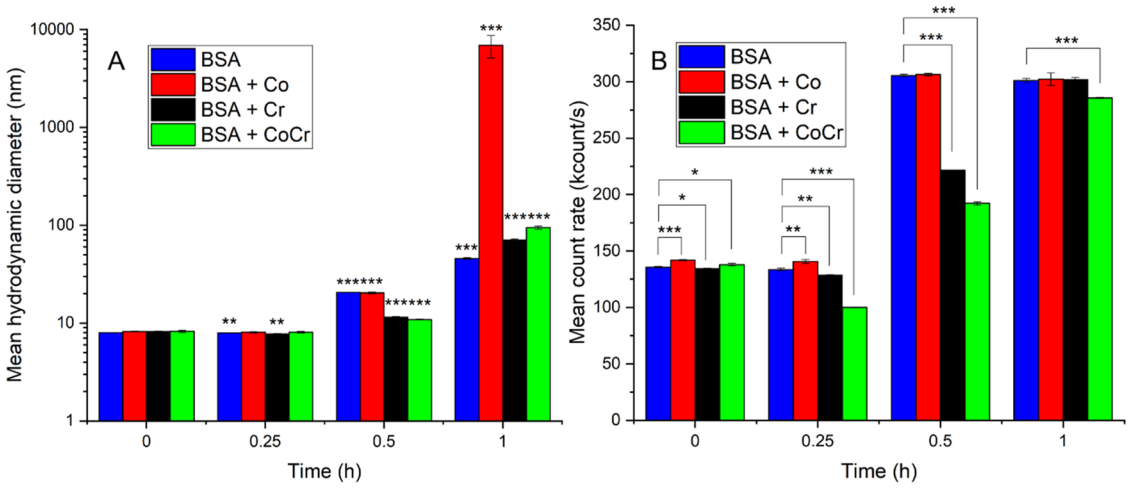

Figure 6. (A) Size statistics for surface-mean diameters of BSA with and without metal ions for different 80 °C heating times (*, $p \leq 0.05$; **, $p \leq 0.01$; ***, $p \leq 0.001$ as compared to the respective samples at 0 h of incubation). (B) Count-rate statistics of BSA with and without metal ions for different 80 °C heating times (*$p \leq 0.05$; **$p \leq 0.01$; ***$p \leq 0.001$).

CD data that indicates Co^{II} ions are destabilizing BSA. In contrast, at the 0.5 h time point, the Cr^{III} solution and the $Co^{II}Cr^{III}$ mixture both possessed smaller average particle size than the native BSA solution ($p < 0.001$). This may be attributed to their stabilizing effects, as seen by CD, or immediate precipitation of larger aggregates.

All metal conditions (Co^{II}, Cr^{III}, and $Co^{II}Cr^{III}$) also immediately resulted in the formation of small peaks around the 100−10,000 nm range (Figure 5B−D). These were only visible in metal-containing BSA solutions, which suggests that all of the tested metal ions may immediately result in a small degree of aggregation. These large-scale aggregates have been discussed before,[18] and are suspected to nearly immediately precipitate, which is why their presence is so inconsistent among DLS measurements. This can also be seen by observing the mean count rate (Figure 6B). The Cr^{III} and $Co^{II}Cr^{III}$ conditions both showed reduced count rates at the 0.25 and 0.5 h mark, which was attributed to the aggregation and immediate precipitation of these short-lived (in solution) aggregates. Therefore, despite their stabilizing effects, Cr^{III} and $Co^{II}Cr^{III}$ are also responsible for some degree of aggregation and thus also display a larger mean hydrodynamic diameter than the native BSA solution after 1 h (Figure 6A). This is suggested to be due to the Coulombic attraction between the positively charged metal ions and negatively charged protein functional groups causing several proteins to agglomerate around the metal ions. These results support our previous findings,[18] as the trivalent metal ion seems to cause more immediate aggregation than the divalent metal ion, and the mixture results in the greatest amount of these large-sized peaks and the lowest count rate (Figure 6B).

Co^{II} ions had a clear ability to induce aggregation, as seen by the large size distribution after one h at 80 °C and in the reduction in melting temperature by circular dichroism. While Cr^{III} and $Co^{II}Cr^{III}$ could reduce aggregation, after 1 h at 80 °C, these effects were ultimately overshadowed by the high degree of thermal aggregation and the salt bridging of metal ions.

3.5. ζ-Potential. The addition of metal ions reduced the ζ-potential to more positive values (less negative charge), regardless of the metal ion identity (Table 1).

Despite Cr^{III} existing in solution as the negatively charged $Cr(C_2O_4)_3^{3-}$ complex, the mean ζ-potential of BSA in chromium-containing solutions was more positive than the ζ-potential of native BSA. This suggests that Cr is not binding to BSA as the negatively charged oxalate but as a positively charged ion, where the oxalate ligands are likely exchanged for functional groups of the protein, which supports the suggested mechanism of metal-induced protein aggregation being salt bridging.

Table 1. High-Conductivity (150 mM NaCl) ζ-Potential of 8:1 Metal/Protein Solutions[a]

sample	mean ζ-potential (mV)
BSA	−17.2 ± 0.94
BSA + Co^{II}	−11.7 ± 0.40
BSA + Cr^{III}	−13.2 ± 1.52
BSA + $Co^{II}Cr^{III}$	−10.7 ± 2.26

[a] $p < 0.001$ for all measurements compared to metal-free BSA.

Our ζ-potential investigation has been carried out at 150 mM NaCl, which is not comparable to literature data at lower ionic strength.[45,46] An investigation into the ζ-potential of BSA and BSA with metal ions was additionally carried out (Figure 7) using buffers of 20 mM MES adjusted to pH 7.3, with four NaCl concentrations: 1, 50, 100, and 150 mM. The ζ-potential of BSA became more negative as the salt concentration was increased; Co^{II}-containing solutions had approximately the same ζ-potential at all ionic strengths; and Cr^{III}-containing solutions had a very negative ζ-potential at low ionic strength, which became more positive with increasing ionic strength. The effects of salt concentration on protein interactions have been widely studied; salt molecules raise the surface tension of the solution, diminish the electrostatic interaction between suspension molecules, and alter the surface activity of protein molecules. However, this remains a complex area of study due to the intricacy of competing forces and interactions.[46,47] Previous investigations suggest that increasing the salt concentration should result in a more positive ζ-potential of BSA, which is the opposite of what is observed in our case, although none of the experiments used buffered solutions of BSA when taking ζ-potential measurements.[46,48,49] It is possible in our case that the MES buffer influenced the ζ-potential of the protein colloids. At low ionic strengths, it is possible that Cr^{III} binds as an ion to BSA, and the oxalate

https://doi.org/10.1021/acsabm.3c00463
ACS Appl. Bio Mater. 2023, 6, 3832−3841

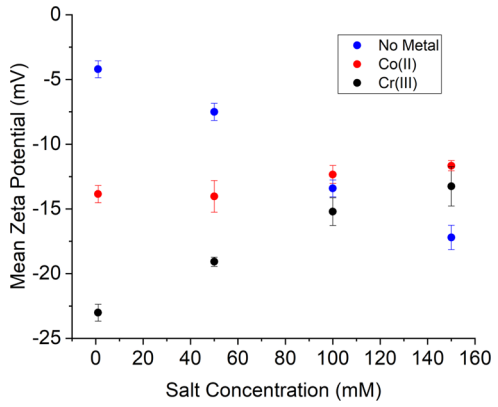

Figure 7. ζ-Potential measurement of BSA and BSA containing 8:1 metal/protein ratio of Co^{II} (from $CoCl_2$ salt) and Cr^{III} (from potassium chromium oxalate salt) in varying NaCl concentrations, buffered with 20 mM MES buffer to pH 7.3 and analyzed after 2 h at 37 °C.

counterions adsorb and help stabilize charges on the surface of BSA, reducing the effecting ζ-potential. As the ionic strength increases, the oxalate does not adsorb to BSA, as the charged residues are already surrounded by solvated chloride counterions—Cl^- is an indifferent electrolyte to BSA and would not impact the ζ-potential, leading to the more positive value that is observed.[46] These complex observations will require more investigations to fully understand. It is, however, clear that the metal ions interact with the BSA at all ionic strength values investigated and alter its ζ-potential.

4. FURTHER DISCUSSION

Most systematic studies of metal-induced protein aggregation are inspired by the involvement of some metal ions in the development of neurodegenerative diseases, naturally, the focus of these investigations is on biogenic metals; metals found within living organisms, or more specifically the metals found within the human brain and nervous system.[50,51] Iron, copper, and zinc are the three most abundant trace metals in the human brain,[51] and these metals are the subject of much investigation simply because they are more likely associated with these diseases.[50−54] Some investigations are also carried out on noble metals, platinum, gold, and silver due to their recent applications as anticancer complexes,[53,55] and aluminum due to its huge abundance in the earth's crust and presence in contaminated drinking water and processed foods.[56] There is a paucity of systematic studies investigating the impacts of common alloying elements such as Co and Cr on the aggregation of proteins, despite their prevalence in biomedical implants, tool steels, cooking implements, and food/drug manufacturing equipment, all of which are potential routes of exposure.

The consensus in the literature is that metals and metalloids may influence the aggregation properties of proteins and may promote certain neurodegenerative diseases through largely unknown mechanisms.[57−60] Previous investigation into the impacts of Cr^{III} on the conformational stability of BSA suggests that the addition of metal results in the partial unfolding of the protein.[61] This result is not supported by the findings presented in this paper; the presence of a partially unfolded structural state was not detected. A likely cause for this discrepancy was the choice of the chromium salt used in the initial investigation. Chromium chloride is not stable at physiological pH according to Hydra/Medusa chemical equilibrium software,[39] and its addition to a buffered solution will result in the formation of solid Cr_2O_3 or $Cr(OH)_3$ particles.[62] These nanoparticles are suspected to result in a greater extent of protein aggregation and may result in the formation of partially unfolded protein structures—this is an area that requires further investigation.[63] It is also possible the addition of $CrCl_3$ resulted in acid-induced unfolding of BSA, as aqueous Cr^{III} is stable at low pH in the form of $Cr_3(OH)_4^{5+}$ or free Cr^{3+} (see Section S5 in the Supporting Information) and $CrCl_3$ acidified the aqueous solution. Another study determined that Cr^{III} leads to aggregation of human serum albumin; however, no conclusive evidence was presented to suggest a mechanism-the authors speculated that Cr^{III} ions could form bridges between the albumin molecules, for example via a dimeric chromium-hydroxy complex.[64] This salt-bridging effect is the mechanism suggested in this paper.

There is a research gap regarding the formation of the protein aggregates that immediately precipitate from solution, even though large precipitated aggregates are likely the ones that are most harmful to human health or adsorb to metal surfaces, resulting in modified corrosion properties. It is unclear if the formation of these particles *in vitro* is caused by a chemical impurity or a nucleation process that would also be relevant *in vivo*. Purchased BSA undergoes multiple purification steps to remove fatty acids and surfactants; however, it has been reported that high-molecular-weight contaminants may be found within high-purity BSA.[65] This contaminant is likely another larger protein. Although no impurities were detected in our system, it is possible that the formation of these aggregates is impurity-driven. Additionally, in this study, temperature was used as an accelerator in a variety of ways. A water bath at 90 °C was used to thermally unfold BSA for ICP-MS analysis, and an 80 °C oven was used to aggregate BSA for particle size distribution analysis. This elevated temperature may alter the way metal ions interact with BSA, and the results presented here may not be representative of the interplay between components under physiological conditions.

Byproducts from metals undergoing both physical wear processes and corrosion (tribocorrosion) result in the production of more than just metal ions: metal wear debris and nanoparticles are also released into the surrounding environment.[21] These materials are also implicated in protein aggregation,[63] and the biotribocorrosion of metallic implants is widely studied.[66,67] These tribocorrosion products may be ingested by local cells including macrophages, dendritic cells, osteoclasts, and osteoblasts, and disseminated throughout the body.[21] To comprehensively understand the phenomenon of metal-induced protein aggregation, more work is required to elucidate the impact of these solid metal nanoparticles on the protein stability.

5. CONCLUSIONS

This study investigated BSA aggregation in the presence of Co^{II}, Cr^{III}, and an equimolar mixture of the two at pH 7.3 and varying molar metal/protein ratios, as our hypothesis was that Co and Cr ions accelerate the aggregation of BSA via a salt-bridging mechanism. It was determined that metal ions under physiological conditions were preferentially incorporated into thermally unfolded protein aggregates. Co^{II} had a destabilizing effect on BSA's structure, while Cr^{III} and the $Co^{II}Cr^{III}$ mixture had stabilizing effects. All metal ions had the potential to induce large protein aggregates, visible immediately upon the

https://doi.org/10.1021/acsabm.3c00463
ACS Appl. Bio Mater. 2023, 6, 3832−3841

addition of metal, that immediately precipitated from solution without incubation at elevated temperature. The mechanism for metal-induced protein aggregation was found to be salt bridging, where multiple proteins chelate metal ions, resulting in a large tangle of metals and proteins. Despite being insoluble at physiological pH, Cr^{III} was found to bind to BSA as a cation, not as the soluble Cr^{III} oxalate complex at 150 mM NaCl concentration. These results are consistent with other findings, that both Co^{II} and Cr^{III} ions can induce albumin aggregation,[10,37,61,64] confirming our hypothesis. These research findings will help ameliorate the study of corrosion in biological environments as well as improve safety standards for biomedical implants, although more work is required to determine the impact of Co^{II} and Cr^{III} nanoparticles on protein stability.

■ ASSOCIATED CONTENT

Data Availability Statement

Raw data is available on the platform Open Science Framework (https://osf.io/895n3/?view_only=bfccf2e4998d41a4acfe99b0d66471d1).

Supporting Information

The Supporting Information is available free of charge at https://pubs.acs.org/doi/10.1021/acsabm.3c00463.

Details of additional experiments investigating $Co(OH)_2$ nanoparticle formation, speciation modeling, experimental schemas, and additional experimental details (PDF)

■ AUTHOR INFORMATION

Corresponding Authors

Zoltan Wolfgang Richter-Bisson − *Department of Chemistry, Western University, London, ON N6A 5B7, Canada;* orcid.org/0009-0004-6056-6003; Email: zrichter@uwo.ca

Yolanda Susanne Hedberg − *Department of Chemistry, Western University, London, ON N6A 5B7, Canada; Surface Science Western, Western University, London, ON N6G 0J3, Canada; Lawson Health Research Institute, London, ON N6C2R5, Canada;* orcid.org/0000-0003-2145-3650; Phone: (+1) (519) 661-2111; Email: yhedberg@uwo.ca

Author

Aleksandra Doktor − *Department of Chemistry, Western University, London, ON N6A 5B7, Canada*

Complete contact information is available at: https://pubs.acs.org/10.1021/acsabm.3c00463

Author Contributions

Z.W.R.-B.: conceptualization, methodology, validation, formal analysis, investigation, writing—original draft preparation, visualization, supervision, funding acquisition; A.D.: investigation, visualization; Y.S.H.: conceptualization, methodology, resources, writing—review & editing, visualization, supervision, project administration, funding acquisition.

Notes

The authors declare no competing financial interest.

■ ACKNOWLEDGMENTS

Lee-Ann Briere and Dr. Lars Konermann, both at the University of Western Ontario, are acknowledged for experimental help and input. Yolanda Hedberg reports financial support was provided by Canada Research Chairs Program (CRC-2019-00425), Natural Sciences and Engineering Research Council of Canada (RGPIN-2021-03997, and DGDND-2021-03997), Taiho Kogyo Tribology Research Foundation (20B04), Canada Foundation for Innovation (42507), and Ontario Ministry of Colleges and Universities (42507). Zoltan Richter-Bisson reports financial support was provided by Ontario Ministry of Colleges and Universities (QEII OGS).

■ REFERENCES

(1) Mishra, S.; Bharagava, R. N.; More, N. S.; Yadav, A.; Zainith, S.; Mani, S.; Chowdhary, P. Heavy Metal Contamination: An Alarming Threat to Environment and Human Health. In *Environmental Biotechnology: For Sustainable Future*; Springer, 2018; p 103.

(2) Cui, Y.; Zhu, Y.-G.; Zhai, R.; Huang, Y.; Qiu, Y.; Liang, J. Exposure to Metal Mixtures and Human Health Impacts in a Contaminated Area in Nanning, China. *Environ. Int.* **2005**, *31* (6), 784−790.

(3) Rabajczyk, A.; Zielecka, M.; Porowski, R.; Hopke, P. K. Metal Nanoparticles in the Air: State of the Art and Future Perspectives. *Environ. Sci. Nano* **2020**, *7*, 3233−3254.

(4) Garner, L. A. Contact Dermatitis to Metals. *Dermatol. Ther.* **2004**, *17*, 321−327.

(5) Münch, H. J.; Jacobsen, S. S.; Olesen, J. T.; Menné, T.; Soballe, K.; Johansen, J. D.; Thyssen, J. P. The Association between Metal Allergy, Total Knee Arthroplasty, and Revision. *Acta Orthop.* **2015**, *86* (3), 378−383.

(6) Pandit, H.; Glyn-Jones, S.; Mclardy-Smith, P.; Gundle, R.; Whitwell, D.; Gibbons, C. L. M.; Ostlere, S.; Athanasou, N.; Gill, H. S.; Murray, D. W. Pseudotumours Associated with Metal-on-Metal Hip Resurfacings. *J. Bone Jt. Surg., Br. Vol.* **2008**, *90* (7), 847−851.

(7) Wagner, P.; Olsson, H.; Lidgren, L.; Robertsson, O.; Ranstam, J. Increased Cancer Risks among Arthroplasty Patients: 30 Year Follow-up of the Swedish Knee Arthroplasty Register. *Eur. J. Cancer* **2011**, *47* (7), 1061−1071.

(8) Rajan, R.; Ahmed, S.; Sharma, N.; Kumar, N.; Debas, A.; Matsumura, K. Review of the Current State of Protein Aggregation Inhibition from a Materials Chemistry Perspective: Special Focus on Polymeric Materials. *Mater. Adv.* **2021**, *2*, 1139−1176, DOI: 10.1039/d0ma00760a.

(9) Chen, J. K.; Thyssen, J. P. *Metal Allergy*; Springer International Publishing, 2018.

(10) Hedberg, Y. S.; Pettersson, M.; Pradhan, S.; Odnevall Wallinder, I.; Rutland, M. W.; Persson, C. Can Cobalt(II) and Chromium(III) Ions Released from Joint Prostheses Influence the Friction Coefficient? *ACS Biomater. Sci. Eng.* **2015**, *1* (8), 617−620.

(11) Lee, S.; Choi, M. C.; Al Adem, K.; Lukman, S.; Kim, T. Y. Aggregation and Cellular Toxicity of Pathogenic or Non-Pathogenic Proteins. *Sci. Rep* **2020**, *10* (1), No. 5120, DOI: 10.1038/s41598-020-62062-3.

(12) Poulson, B. G.; Szczepski, K.; Lachowicz, J. I.; Jaremko, L.; Emwas, A. H.; Jaremko, M. Aggregation of Biologically Important Peptides and Proteins: Inhibition or Acceleration Depending on Protein and Metal Ion Concentrations. *RSC Adv.* **2019**, *10*, 215−227, DOI: 10.1039/C9RA09350H.

(13) Cunat, P.-J. *Alloying Elements in Stainless Steel and other Chromium-Containing Alloys 2004*; Euro Inox: Paris, 2004.

(14) Hedberg, Y. S.; Odnevall Wallinder, I. Metal Release from Stainless Steel in Biological Environments: A Review. *Biointerphases* **2016**, *11* (1), No. 018901.

(15) Milošev, I. From in Vitro to Retrieval Studies of Orthopedic Implants. *Corrosion* **2017**, *73* (12), 1496−1509.

(16) Okazaki, Y.; Gotoh, E. Metal Release from Stainless Steel, Co-Cr-Mo-Ni-Fe and Ni-Ti Alloys in Vascular Implants. *Corros. Sci.* **2008**, *50* (12), 3429−3438.

(17) Ackland, M. L.; Bornhorst, J.; Dedoussis, G. V.; Dietert, R. R.; Nriagu, J. O.; Pacyna, J. M.; Pettifor, J. M. *Trace Metals and Infectious Diseases: Metals in the Environment as Risk Factors for Infectious*

Diseases; Nriagu, J. O.; Skaar, E. P., Eds.; MIT Press: Cambridge, 2015.
(18) Hedberg, Y. S.; Dobryden, I.; Chaudhary, H.; Wei, Z.; Claesson, P. M.; Lendel, C. Synergistic Effects of Metal-Induced Aggregation of Human Serum Albumin. *Colloids Surf., B* **2019**, *173*, 751−758.
(19) Antony, K. C. Wear-Resistant Cobalt-Base Alloys. *J. Miner., Met. Mater. Soc.* **1983**, *35*, 52−60.
(20) Al Jabbari, Y. S. Physico-Mechanical Properties and Prosthodontic Applications of Co-Cr Dental Alloys: A Review of the Literature. *J. Adv. Prosthodontics* **2014**, *6* (2), 138−145.
(21) Wu, D.; Bhalekar, R. M.; Marsh, J. S.; Langton, D. J.; Stewart, A. J. Periarticular Metal Hypersensitivity Complications of Hip Bearings Containing Cobalt−Chromium. *EFORT Open Rev.* **2022**, *7* (11), 758−771.
(22) Hartmann, A.; Hannemann, F.; Lützner, J.; Seidler, A.; Drexler, H.; Günther, K.-P.; Schmitt, J. Metal Ion Concentrations in Body Fluids after Implantation of Hip Replacements with Metal-on-Metal Bearing—Systematic Review of Clinical and Epidemiological Studies. *PLoS One* **2013**, *8* (8), No. e70359.
(23) Bal, W.; Sokołowska, M.; Kurowska, E.; Faller, P. Binding of Transition Metal Ions to Albumin: Sites, Affinities and Rates. *Biochim. Biophys. Acta, Gen. Subj.* **2013**, *1830*, 5444−5455.
(24) Hassan, M.; Azzazy, E.; Christenson, R. H. All About Albumin: Biochemistry, Genetics, and Medical Applications. *Clin. Chem.* **1997**, *43* (10), 2014a−22015.
(25) Ghosh, S. K.; Choudhury, D.; Das, N.; Pingguan-Murphy, B. Tribological Role of Synovial Fluid Compositions on Artificial Joints a Systematic Review of the Last 10 Years. *Lubr. Sci.* **2014**, *26*, 387−410.
(26) Barbosa, L. R. S.; Ortore, M. G.; Spinozzi, F.; Mariani, P.; Bernstorff, S.; Itri, R. The Importance of Protein-Protein Interactions on the PH-Induced Conformational Changes of Bovine Serum Albumin: A Small-Angle x-Ray Scattering Study. *Biophys. J.* **2010**, *98* (1), 147−157.
(27) Oates, K. M. N.; Krause, W. E.; Jones, R. L.; Colby, R. H. Rheopexy of Synovial Fluid and Protein Aggregation. *J. R. Soc. Interface* **2006**, *3* (6), 167−174.
(28) Aleksić, M.; Pease, C. K. S.; Basketter, D. A.; Panico, M.; Morris, H. R.; Dell, A. Investigating Protein Haptenation Mechanisms of Skin Sensitisers Using Human Serum Albumin as a Model Protein. *Toxicol. In Vitro* **2007**, *21* (4), 723−733.
(29) Topală, T.; Bodoki, A.; Oprean, L.; Oprean, R. Bovine Serum Albumin Interactions with Metal Complexes. *Clujul Med.* **2014**, *87* (4), 215−219.
(30) Klok, O.; Munoz, A. I.; Mischler, S. An Overview of Serum Albumin Interactions with Biomedical Alloys. *Materials* **2020**, *13*, No. 4858, DOI: 10.3390/ma13214858.
(31) Yu, X.; Qu, H.; Knecht, D. A.; Wei, M. Incorporation of Bovine Serum Albumin into Biomimetic Coatings on Titanium with High Loading Efficacy and Its Release Behavior. *J. Mater. Sci. Mater. Med.* **2009**, *20* (1), 287−294.
(32) Shard, A. G.; Tomlins, P. E. Biocompatibility and the Efficacy of Medical Implants. *Regener. Med.* **2006**, *1* (6), 789−800.
(33) Lemire, J. A.; Harrison, J. J.; Turner, R. J. Antimicrobial Activity of Metals: Mechanisms, Molecular Targets and Applications. *Nat. Rev. Microbiol.* **2013**, *11*, 371−384.
(34) Tamás, M.; Sharma, S. K.; Ibstedt, S.; Jacobson, T.; Christen, P. Heavy Metals and Metalloids as a Cause for Protein Misfolding and Aggregation. *Biomolecules* **2014**, *4*, 252−267.
(35) Beyersmann, D.; Hartwig, A. Carcinogenic Metal Compounds: Recent Insight into Molecular and Cellular Mechanisms. *Arch. Toxicol.* **2008**, *82* (8), 493−512.
(36) Banfalvi, G. *Cellular Effects of Heavy Metals*; Springer: Dordrecht, Netherlands, 2011. DOI: 10.1007/978-94-007-0428-2.
(37) Yang, J.; Black, J. Competitive Binding of Chromium, Cobalt and Nickel to Serum Proteins. *Biomaterials* **1994**, *15*, 262−268, DOI: 10.1016/0142-9612(94)90049-3.
(38) Meachim, G.; Williams, D. F. Changes in Nonosseous Tissue Adjacent to Titanium Implants. *J. Biomed Mater. Res.* **1973**, *7* (6), 555−572.
(39) Puigdomenech, I. *Hydra/Medusa Chemical Equilibrium Database and Plotting Software*; KTH Royal Institute of Technology: Stockholm, 2015.
(40) Verma, A. K.; Kore, R.; Corbin, D. R.; Shiflett, M. B. Metal Recovery Using Oxalate Chemistry: A Technical Review. *Ind. Eng. Chem. Res.* **2019**, *58*, 15381−15393, DOI: 10.1021/acs.iecr.9b02598.
(41) Swint, L.; Robertson, A. D. *Thermodynamics of Unfolding for Turkey Ovomucoid Third Domain: Thermal and Chemical Denaturation*; Cambridge University Press, 1993; Vol. *2*. DOI: 10.1002/pro.5560021205.
(42) Soliman, M. Y. M.; Medema, G.; Bonilla, B. E.; Brouns, S. J. J.; van Halem, D. Inactivation of RNA and DNA Viruses in Water by Copper and Silver Ions and Their Synergistic Effect. *Water Res.: X* **2020**, *9*, No. 100077.
(43) Alexandrov, P. N.; Zhao, Y.; Pogue, A. I.; Tarr, M. A.; Kruck, T. P. A.; Percy, M. E.; Cui, J.-G.; Lukiw, W. J. Synergistic Effects of Iron and Aluminum on Stress-Related Gene Expression in Primary Human Neural Cells. *J. Alzheimer's Dis.* **2005**, *8*, 117−127.
(44) Eichler, T. E. Differential Induction of Podocyte Heat Shock Proteins by Prolonged Single and Combination Toxic Metal Exposure. *Toxicol. Sci.* **2005**, *84* (1), 120−128.
(45) Ravindran, S.; Williams, M. A. K.; Ward, R. L.; Gillies, G. Understanding How the Properties of Whey Protein Stabilized Emulsions Depend on PH, Ionic Strength and Calcium Concentration, by Mapping Environmental Conditions to Zeta Potential. *Food Hydrocolloids* **2018**, *79*, 572−578.
(46) Salgın, S.; Salgin, U.; Bahadir, S. Zeta Potentials and Isoelectric Points of Biomolecules: The Effects of Ion Types and Ionic Strengths. *Int. J. Electrochem. Sci.* **2012**, *7*, 12404−12414.
(47) Chen, W. Y.; Liu, Z. C.; Lin, P. H.; Fang, C. I.; Yamamoto, S. The Hydrophobic Interactions of the Ion-Exchanger Resin Ligands with Proteins at High Salt Concentrations by Adsorption Isotherms and Isothermal Titration Calorimetry. *Sep. Purif. Technol.* **2007**, *54* (2), 212−219.
(48) Grisham, D. R.; Nanda, V. Zeta Potential Prediction from Protein Structure in General Aqueous Electrolyte Solutions. *Langmuir* **2020**, *36* (46), 13799−13803.
(49) Salgın, S. Effects of Ionic Environments on Bovine Serum Albumin Fouling in a Cross-Flow Ultrafiltration System. *Chem. Eng. Technol.* **2007**, *30* (2), 255−260.
(50) Navarra, G.; Tinti, A.; Leone, M.; Militello, V.; Torreggiani, A. Influence of Metal Ions on Thermal Aggregation of Bovine Serum Albumin: Aggregation Kinetics and Structural Changes. *J. Inorg. Biochem.* **2009**, *103* (12), 1729−1738.
(51) Everett, J.; Lermyte, F.; Brooks, J.; Tjendana-Tjhin, V.; Plascencia-Villa, G.; Hands-Portman, I.; Donnelly, J. M.; Billimoria, K.; Perry, G.; Zhu, X.; Sadler, P. J.; O'connor, P. B.; Collingwood, J. F.; Telling, N. D. Biogenic Metallic Elements in the Human Brain? *Sci. Adv.* **2021**, *7*, 6707−6716.
(52) Petoukhov, M. V.; Sokolov, A. V.; Kostevich, V. A.; Samygina, V. R. Copper-Induced Oligomerization of Ceruloplasmin. *Crystallogr. Rep.* **2021**, *66* (5), 828−832.
(53) Alhazmi, H. A.; Ahsan, W.; Ibrahim, A. M. M.; Khubrani, R. A. Y.; Haddadi, Z. A. A.; Safhi, A. Y. F.; Shubayr, N.; Al Bratty, M.; Najmi, A. Investigation of Bovine Serum Albumin Aggregation upon Exposure to Silver(i) and Copper(Ii) Metal Ions Using Zetasizer. *Open Chem.* **2021**, *19* (1), 987−997.
(54) San Biago, P. L.; Bulone, D. *Biophysical Inquiry into Protein Aggregation and Amyloid Diseases*; Transworld Research Network: Trivandrum, Kerala, India, 2008.
(55) Zhang, H.; Zhang, M.; Wang, Y.; Wang, Y.; Sun, S.; Fei, Z.; Cao, J. Effects of Selected Two Noble Metal Ions in Medicine on the Structure and Activity of Bovine Serum Albumin: A Multi-Spectral Studies. *J. Lumin.* **2018**, *194*, 519−529.
(56) Shahnawaz Khan, M.; Tabrez, S.; Rehman, M. T.; Alokail, M. S. Al (III) Metal Augment Thermal Aggregation and Fibrillation in

Protein: Role of Metal Toxicity in Neurological Diseases. *Saudi J. Biol. Sci.* **2020**, *27* (9), 2221−2226.
(57) Breydo, L.; Uversky, V. N. Role of Metal Ions in Aggregation of Intrinsically Disordered Proteins in Neurodegenerative Diseases. *Metallomics* **2011**, *3* (11), 1163−1180.
(58) Alies, B.; Hureau, C.; Faller, P. The Role of Metal Ions in Amyloid Formation: General Principles from Model Peptides. *Metallomics* **2013**, *5* (3), 183−192.
(59) Greenough, M. A.; Camakaris, J.; Bush, A. I. Metal Dyshomeostasis and Oxidative Stress in Alzheimer's Disease. *Neurochem. Int.* **2013**, *62* (5), 540−555.
(60) Caudle, W. M.; Guillot, T. S.; Lazo, C. R.; Miller, G. W. Industrial Toxicants and Parkinson's Disease. *Neurotoxicology* **2012**, *33*, 178−188.
(61) Chen, M.; Liu, Y.; Cao, H.; Song, L.; Zhang, Q. The Secondary and Aggregation Structural Changes of BSA Induced by Trivalent Chromium: A Biophysical Study. *J. Lumin.* **2015**, *158*, 116−124.
(62) Beverskog, B.; Puigdomenech, I. Revised Pourbaix Diagrams for Chromium at 25−300 °C. *Corros. Sci.* **1997**, *39* (1), 43−57.
(63) Zaman, M.; Ahmad, E.; Qadeer, A.; Rabbani, G.; Khan, R. H. Nanoparticles in Relation to Peptide and Protein Aggregation. *Int. J. Nanomed.* **2014**, 899−912.
(64) Österberg, R.; Sjöberg, B.; Persson, D. Cr(III)-Induced Polymerization of Human Albumin. *Biol. Trace Elem. Res.* **1981**, *3* (3), 157−167.
(65) Gu, J. H.; Qian, R.; Chou, R.; Bondarenko, P. V.; Goldenberg, M. Rotational Rheology of Bovine Serum Albumin Solutions: Confounding Effects of Impurities, Mechanistic Considerations and Potential Implications on Protein Formulation Development. *Pharm. Res.* **2018**, *35* (8), 157.
(66) Thompson, C.; Wilson, K.; Kim, Y. J.; Xie, M.; Wang, W. K.; Wendeler, M. Impact of Magnetic Stirring on Stainless Steel Integrity: Effect on Biopharmaceutical Processing. *J. Pharm. Sci.* **2017**, *106* (11), 3280−3286.
(67) Taufiqurrakhman, M.; Neville, A.; Bryant, M. In *Factors Influencing the Bio-Tribo-Corrosion and Chemistry on Cobalt Alloys: A Brief Literature Review*, AIP Conference Proceedings, American Institute of Physics Inc., 2022.

https://doi.org/10.1021/acsabm.3c00463
ACS Appl. Bio Mater. 2023, 6, 3832−3841